An energy approach for assessing seismic liquefaction potential

Law, K. T.; Cao, Y. L.; He, G. N.

Publisher's version / Version de l'éditeur:
https://doi.org/10.4224/40001226
Paper (National Research Council of Canada. Institute for Research in Construction), 1990-06

National Research Council Canada
Conseil national de recherches Canada

Canada

Reprinted from

Réimpression de la

Canadian Geotechnical Journal

Revue canadienne de géotechnique

An energy approach for assessing seismic liquefaction potential

K. T. LAW, Y. L. CAO, AND G. N. HE

Volume 27 • Number 3 • 1990

Pages 320–329

NRCC 31593

(IRC Paper 1657)

Printed in Canada / Imprimé au Canada

An energy approach for assessing seismic liquefaction potential

K. T. LAW AND Y. L. CAO

Geotechnical Section, Institute for Research in Construction, National Research Council of Canada, Ottawa, Ont., Canada K1A 0R6

AND

G. N. HE

Department of Civil Engineering, Dalian University of Technology, Dalian, China

Received May 26, 1989

Accepted January 15, 1990

An energy method for assessing liquefaction potential of granular soils was developed based on laboratory tests and observational data obtained in past major earthquakes. Cyclic triaxial and cyclic simple shear tests were conducted and the results show that a unique relation exists between the dissipated energy during cyclic load and the excess pore pressure that eventually led to liquefaction failure. This unique relation has been combined with an energy attenuation equation to develop a criterion for defining the liquefaction potential of a site. Parameters for the criterion were evaluated from 136 sites involved in 13 major earthquakes over the world. A comparison was made between the energy method and the commonly used stress method. The energy method was found to be simpler to apply and more reliable.

Key words: energy, earthquake, liquefaction potential, standard penetration test, laboratory cyclic test, excess pore pressure, granular soils, case records.

Une méthode basée sur l'énergie pour évaluer le potentiel de liquéfaction des sols pulvérulents a été développée à partir d'essais en laboratoire et de données d'observation obtenues au cours des principaux tremblements de terre antérieurs. Des essais triaxiaux cycliques et des essais de cisaillement simple cycliques ont été faits, et les résultats démontrent qu'il existe une relation unique entre l'énergie dissipée au cours du chargement cyclique et l'excédent de pression interstitielle qui conduit éventuellement à la rupture en liquéfaction. Cette relation unique a été combinée avec une équation d'atténuation d'énergie pour définir un critère de liquéfaction potentielle d'un site. Des paramètres pour le critère ont été évalués à partir de 136 sites impliqués dans 13 tremblements de terre majeurs à travers le monde. La méthode de l'énergie a été comparée avec la méthode de contrainte plus couramment utilisée. Il a été observé que la méthode de l'énergie est plus simple à utiliser et plus fiable.

Mots clés : énergie, tremblement de terre, potentiel de liquéfaction, essai de pénétration standard, essai cyclique en laboratoire, pression interstitielle, sols pulvérulents, histoire de cas.

[Traduit par la revue]

Can. Geotech. J. **27**, 320–329 (1990)

Introduction

Soil liquefaction may arise when saturated granular or cohesionless soils are shaken, resulting in a loss of strength. In this state the soil will behave like a liquid. This will cause building settlement or tipping, sand boils, ground cracks, landslides, dam instability, highway embankment failures, or other hazards. Such damages are generally of great concern to public safety and are of economic significance.

The assessment of the potential for liquefaction due to an earthquake at a site is a complex engineering problem. Many factors influence the mechanism of liquefaction. They include the magnitude and intensity of the earthquake, the seismic attenuation characteristics, the distance from the source of the earthquake, soil type and properties, confining pressure, and other site-specific conditions. Considerable attention has been given to solving this problem and a number of methods now exist for analysis of liquefaction potential.

There are two broad groups of analysis. The first group (Seed and Idriss 1967, 1971) involves estimating the shear stress level likely to develop in the field under a certain design earthquake. Then laboratory tests are conducted on soil samples to determine the liquefaction resistance under the design earthquake. By comparing the induced shear level and the liquefaction resistance, liquefiable zones are identified.

The second group of analysis is based on field observations of performance of sites subjected to earthquakes in the past. Data on earthquake characteristics and soil resistance measured with the standard penetration test are compiled to establish an empirical relationship for new sites. This group can be further divided into two classes. The first class is based on the possible dynamic stress induced at a site under a design earthquake (Iwasaki *et al.* 1978; Seed *et al.* 1983). The second class is based on the dissipated seismic energy (He 1981; Davis and Berrill 1982). Although the first class has been more widely applied, the second class possesses some advantages, which will be described later.

This paper describes a study that builds on the energy concept for assessing the liquefaction potential of a site. By means of laboratory testing, a basic relationship is established between the excess pore pressure that ultimately leads to liquefaction and parameters governing the soil state. This relationship is combined with dissipated seismic energy and the corrected standard penetration resistance to form a simple criterion for evaluating liquefaction potential. Case records of 136 sites were studied and the results show that this energy method is simpler and more reliable than the stress method by Seed *et al.* (1983).

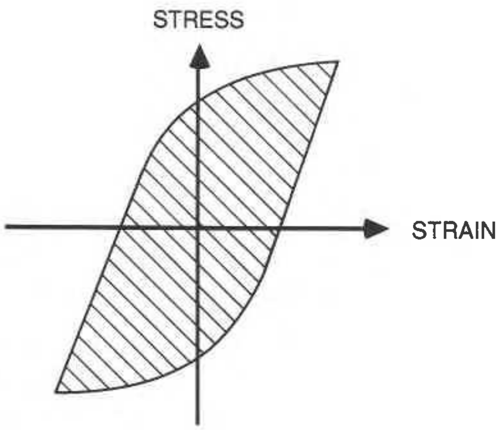

FIG. 1. Hysteretic loop of the soil under cyclic loading.

Development of an energy approach

Soil will deform under vibrations in a hysteretic manner as shown in Fig. 1. During the deformation process, energy will be dissipated. The amount of energy dissipated is commonly represented by the area of the hysteresis loop.

For dry sand, deformation leads to slippage and rearrangement of the sand grains. Consequently, a volumetric change of the soil skeleton will result. If the sand is saturated and if drainage is not permitted during deformation, the tendency of the volumetric change is to cause a transfer of the effective stress from the soil grains to the pore water. An excess pore pressure (Δu) is then generated as proposed by Martin *et al.* (1975):

[1] $\Delta u = E_r \Delta v$

where E_r is the modulus of resilience of the sand and Δv the equivalent volumetric change in a dry state.

As the volumetric change is related to the energy dissipated in the soil (w), [1] can be rewritten as

[2] $\Delta u = E_r F(w)$

or

[3] $\Delta u = G(w)$

where $F(w)$ and $G(w)$ are functions of the dissipated energy. These functions can be experimentally determined.

Experimental study

Fujian standard sand was used for the experimental study. It is a clean medium sand with a uniformity coefficient (C_u) of 1.59, mean effective size (D_{50}) of 0.40 mm, maximum void ratio (e_{max}) of 0.855, and minimum void ratio (e_{min}) of 0.554.

Two test devices were used in the testing program: (1) a cyclic triaxial cell and (2) a cyclic torsional simple shear apparatus. The cyclic triaxial cell tested samples of 80 mm height and 39.1 mm diameter. It used water as cell fluid. The cyclic load was applied with an electromagnetic drive. This device differs from the electropneumatic drive commonly used in North America in that cyclic load of a much larger frequency range (0.1–50 Hz) can be applied. The torsional simple shear apparatus was developed by Tatsuoka *et al.* (1982). It applied horizontal cyclic torque on a hollow cylindrical specimen of 100 mm outer diameter, 60 mm inner diameter, and 100 mm height. The torque was provided via an electropneumatic drive. Again, water was used as the cell fluid to apply the cell pressure.

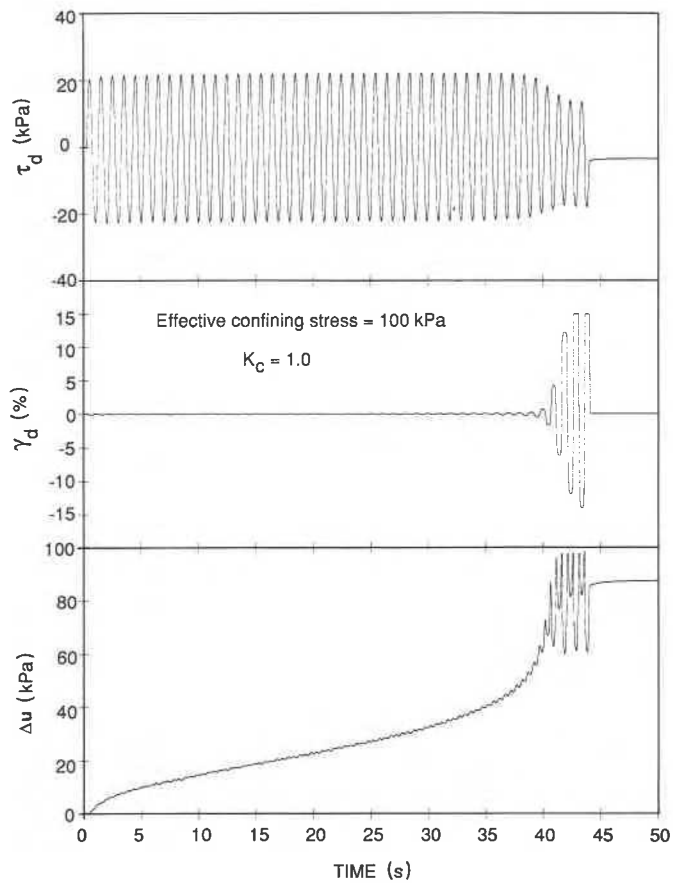

FIG. 2. Typical stress (τ_d), strain (γ_d), and pore pressure (Δu) plots of a cyclic torsional test.

For both test devices, samples were prepared using the moist tamping method in appropriate moulds. The saturation process consisted of passing carbon dioxide through the sample under a small cell pressure to displace the air in the void space. Distilled water was then passed through the sample to replace the carbon dioxide. Any trace of carbon dioxide that remained in the sample would dissolve in the pore water when a back pressure of either 100 or 200 kPa was applied. The pore pressure to confining stress ratio, $\bar{B}$, measured after consolidation was generally in the neighbourhood of 0.95.

Samples were prepared at different relative densities (D_r) and consolidated at different pressures. Both isotropic ($K_c = 1.0$) and anisotropic ($K_c \neq 1.0$) consolidation were used, where K_c is the consolidation ratio defined as $K_c = \sigma'_v/\sigma'_h$, with σ'_v and σ'_h being the consolidation pressure in the vertical and the horizontal direction, respectively. A constant frequency of 1 Hz was maintained in all the tests.

During the undrained cyclic shearing stage, readings were taken via electronic sensors using an IBM PC compatible data acquisition system. For a cycle in the cyclic triaxial test, 40 readings were taken of each of excess pore pressure, vertical cyclic load, and vertical displacement. Similarly, in the torsional simple shear test, 40 readings were taken of each of excess pore pressure, horizontal cyclic torque, horizontal rotation, and vertical displacement. The appropriate readings were processed after the test to define the hysteresis loop for estimating the dissipated energy. The stress, strain, and pore pressure responses during the cyclic triaxial and the

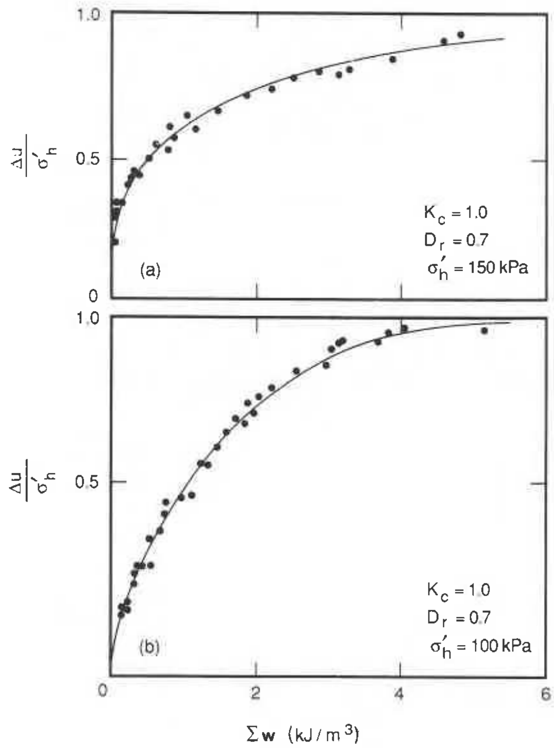

FIG. 3. Typical laboratory test results on Fujian medium sand: (*a*) triaxial tests; (*b*) torsional tests.

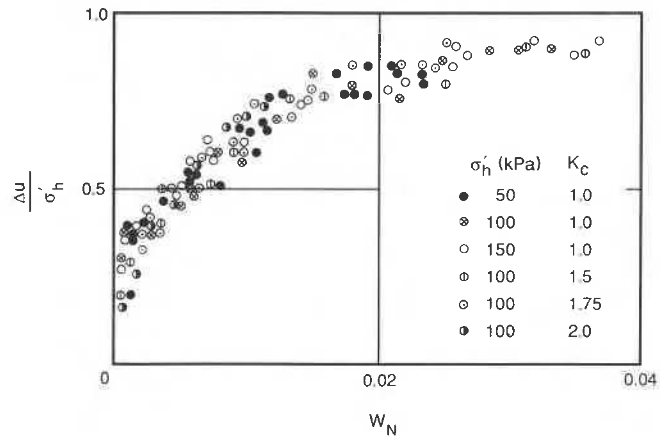

FIG. 4. Normalized excess pore pressure $\Delta u/\sigma'_h$ vs. normalized dissipated energy W_N.

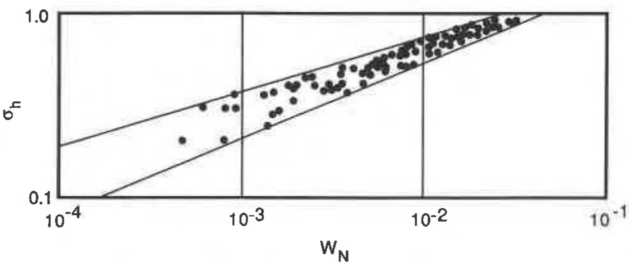

FIG. 5. Normalized excess pore pressure $\Delta u/\sigma'_h$ vs. normalized dissipated energy W_N on a log-log plot.

cyclic torsional simple shear tests are similar to those reported in the open literature for common sand. Typical test result of a cyclic torsional simple shear test are shown in Fig. 2.

A concept of cumulated energy per unit volume ($\Sigma\ w$) is introduced to analyze the test results. This quantity is obtained by the summing of all the areas of the hysteresis loops, represented on a stress–strain plot, after a certain number of load cycles. Figure 3 shows typical test results for both the cyclic triaxial and the torsional simple shear tests. The excess pore pressure Δu normalized by σ'_h is plotted against $\Sigma\ w$ in the figure. The test results show that within reasonable experimental scatter, there exists a functional relationship between $\Delta u/\sigma'_h$ and $\Sigma\ w$.

A normalized dimensionless energy is proposed here to account for the influence of σ'_h, K_c, and D_r. It is expressed as

$$[4] \quad W_N = F_1(K_c)\, F_2(D_r)\, \Sigma\ w/\sigma'_h$$

where $F_1(K_c)$ is the normalizing function to account for K_c and $F_2(D_r)$ is the normalizing function to account for D_r.

Based on statistical analysis of all the test data from the cyclic triaxial tests, F_1 can be given by

$$[5] \quad F_1(K_c) = 1 - \xi \log(K_c)$$

where ξ depends on soil type and test condition. For this case, $\xi = 3.0$.

The function F_2 was determined using the test results from the cyclic torsional simple shear tests and the following is found to be applicable:

$$[6] \quad F_2(D_r) = 10^{\zeta(D_r - 0.70)}$$

where ζ also depends on soil type and test condition and is equal to -2.0 in this test series.

Putting [5] and [6] into [4], one obtains the normalized energy (W_N) corresponding to the normalized excess pressure ($\Delta u/\sigma'_h$) and the results are plotted in Fig. 4. A single functional relationship between these two quantities emerges from the data. To mathematically define the relationship, the results are replotted in Fig. 5 on a log-log scale. This plot shows there is an approximate linear relationship between $\Delta u/\sigma'_h$ and W_N. The relationship can be represented by

$$[7] \quad \frac{\Delta u}{\sigma'_h} = \alpha W_N^{\beta}$$

or by substitution into [4]:

$$[8] \quad \frac{\Delta u}{\sigma'_h} = \alpha[F_1(K_c)\, F_2(D_r)\, \Sigma\ w/\sigma'_h]^{\beta}$$

Equation [8] states that the excess pore pressure under cyclic load for a given sand can be uniquely related to the consolidation pressure, consolidation ratio, relative density, and the cumulative dissipated energy.

For the development in the ensuing sections, this uniqueness is vital, though the exact evaluation of parameters such as ξ, ζ, α, and β is not necessary, as will be illustrated.

Assessment of liquefaction potential at a site

The total energy (E) in joules released from an earthquake of magnitude M on the Richter scale is given by (Gutenberg and Richter 1956)

$$[9] \quad E = 10^{4.8 + 1.5M}$$

This energy equation is chosen here because it has been widely used. Other representations such as that by Street

TABLE 1. Site conditions and earthquake data for liquefaction study (after Seed *et al.* 1975)

No.	Year	Magnitude	Hypocentre distance (km)	Depth of sand (m)	Depth of water table (m)	SPT resistance N	Liquefied(?)	Site
1	1802	6.6	55.6	6.09	0.91	6	No	Niigata
2	1802	6.6	55.6	6.09	0.91	12	No	Niigata
3	1887	6.1	61.5	6.09	0.91	6	No	Niigata
4	1887	6.1	61.5	6.09	0.91	12	No	Niigata
5	1891	8.4	51.7	13.71	0.91	17	Yes	Mino Owari
6	1891	8.4	51.4	9.14	1.82	10	Yes	Mino Owari
7	1891	8.4	51.4	7.62	1.82	19	No	Mino Owari
8	1891	8.4	51.4	6.09	2.43	16	Yes	Mino Owari
9	1925	6.3	15.1	7.62	4.57	3	Yes	Santa Barbara
10	1940	7.0	12.8	4.57	4.57	9	Yes	El Centro
11	1940	7.0	12.8	7.62	6.09	4	Yes	El Centro
12	1940	7.0	12.8	6.10	1.52	1	Yes	El Centro
13	1944	8.3	163.8	3.96	1.52	4	Yes	Tohnankai
14	1944	8.3	163.8	2.44	0.60	1	Yes	Tohnankai
15	1948	7.2	16.3	7.01	3.35	18	Yes	Fukui
16	1948	7.2	16.3	7.01	0.91	28	No	Fukui
17	1948	7.2	16.3	3.05	1.29	3	Yes	Fukui
18	1948	7.2	16.3	6.10	0.91	5	Yes	Fukui
19	1957	5.5	11.9	3.05	2.43	7	Yes	San Francisco
20	1960	8.4	127.9	4.57	3.65	6	Yes	Chile
21	1960	8.4	127.9	4.57	3.65	8	Yes	Chile
22	1960	8.4	127.9	6.10	3.65	18	No	Chile
23	1964	7.5	65.2	6.10	0.91	6	Yes	Niigata
24	1964	7.5	65.2	7.62	0.91	15	Yes	Niigata
25	1964	7.5	65.2	6.10	0.91	12	No	Niigata
26	1964	7.5	65.2	7.62	3.65	6	No	Niigata
27	1964	8.3	102.0	6.10	0.00	5	Yes	Alaska
28	1964	8.3	102.0	6.10	2.43	5	Yes	Alaska
29	1964	8.3	117.7	7.62	0.00	40	No	Alaska
30	1964	8.3	94.5	6.10	6.09	10	Yes	Alaska
31	1964	8.3	65.3	6.10	1.52	13	Yes	Alaska
32	1967	6.3	58.3	0.92	0.92	3	Yes	Caracas
33	1968	7.8	178.1	3.66	0.91	14	No	Ebino
34	1968	7.8	74.7	3.66	0.91	6	Yes	Ebino
35	1968	7.8	178.1	3.05	1.52	15	No	Ebino
36	1968	7.8	162.2	4.57	0.91	6	Yes	Ebino
37	1971	6.6	11.6	6.10	4.58	2	Yes	San Fernando
38	1971	6.6	11.6	16.80	16.80	24	Yes	San Fernando

and Lacroix (1979) are useful for specific regions. Consistent use of one single equation will give rise to some scatter when analyzing the case histories. This will be reflected in the precision of the proposed method to be dealt with in a later section.

Only a fraction of the total energy will arrive at a site away from the earthquake source. Some energy will be dissipated by material attenuation along ray paths and further attenuation will occur because of geometric damping. From studies by Murphy and O'Brien (1977), Hasegawa *et al.* (1981), and Nuttli (1979), the attenuation equation for the seismic energy per unit soil volume arriving at a site (E_I) can be expressed as a function of the hypocentral distance (R):

$$[10] \quad E_I(E, R) = \theta E/R^B$$

where θ is assumed to be a constant and B is a coefficient depending on the properties of the rock through which the seismic waves traverse; its value ranges from 2.5 to 5.0.

A part of the vibration energy arriving at a site (E_I) will be dissipated by the soil found at the site. The amount of dissipated energy per unit volume ($\Sigma\ w$) is dependent on E_I and the soil state at the site. The soil state can be characterized by the relative density and the stress system on the soil, which in turn can be represented by an energy dissipation function λ:

$$[11] \quad \Sigma\ w = \lambda(\sigma_h', K_c, D_r)\ E_I(E, R)$$

The use of [11] may raise two questions. The first deals with soil amplification and the second with the amount of energy reaching the upper part of a soil layer after some energy loss in the lower part.

Soil amplification is the process by which ground motions in certain frequency ranges may be magnified. This is always accompanied by attenuation of ground motions in another frequency range. The stress method for assessing liquefaction potential is based on the maximum peak horizontal acceleration at the ground surface. This implies that some part of ground motions is selectively accounted for while another part is being ignored. This, therefore, constitues a definite deficiency in the stress method. On the other hand, the total energy travelling through and dissipated in a soil media remains unchanged whether part of the motions is amplified or attenuated. The use of the energy approach therefore more adequately accounts for the complete spectrum of ground motions that gives rise to liquefaction failure.

Equation [10] describes the energy arriving at any part of a soil layer. As shown later, the coefficient B is found to be 4.3, a value resulting from the combined effects of geometric damping (in which case $B = 2$) and hysteresis damping. For the upper part of a soil layer, the hypocentral distance will be larger than that of the lower part. The E_I for the upper part, therefore, will be smaller than that for the lower part, indicating an absorption of energy in the lower part. In practice, however, R is in 10's of kilometres and the thickness of the soil layer in 10's of metres; the energy E_I arriving at different depths of the soil layer is therefore not significantly different.

Substituting [9]–[11] into [8], one obtains:

$$[12] \quad \frac{\Delta u}{\sigma_h'} = \alpha\left[\frac{F_1(K_c)\,F_2(D_r)\,\lambda(\sigma_h', K_c, D_r)\,\theta \times 10^{15M+4.8}}{\sigma_h' R^B}\right]^{\beta}$$

The right-hand side of [12] contains functions of σ_h', K_c, and D_r. These functions, along with the constants, can be lumped into a single function, η. To simplify the application of [12], the parameters for η should be chosen on the basis that it can be easily determined and reflects the influence of σ_h', K_c, and D_r (Gibbs and Holtz 1957). It is proposed here to use the resistance from the standard penetration test (SPT) corrected to a standard effective vertical overburden stress (N_1) (Seed *et al.* 1983) and for different energy efficiencies associated with test procedures (Seed *et al.* 1985). Hence η can be represented by

$$[13] \quad \eta(N_1) = \frac{\alpha^{-1/\beta}\sigma_h' \times 10^{-4.8}}{F_1(K_c)\,F_2(D_r)\,\lambda(\sigma_h', K_c, D_r)\,\theta}$$

The use of the effective vertical stress for correcting N values should not be confused with the use of effective horizontal stress for assessing liquefaction potential in the laboratory. The correction is a process by which N values obtained at different depths corresponding to different confining stresses can be compared on a single stress reference. This reference is arbitrary and other references such as the effective horizontal stress could have been used.

Putting [13] into [12] yields

$$[14] \quad \frac{\Delta u}{\sigma_h'} = \left[\frac{10^{1.5M}}{\eta(N_1)\,R^B}\right]^{\beta}$$

For cohesionless soils, the condition of liquefaction is reached when the stress or the *in situ* confining stress (σ_h') is completely transferred to the pore water so that the excess pore pressure is equal to σ_h', i.e., when

$$[15a] \quad \frac{\Delta u}{\sigma_h'} = 1.0$$

or

$$[15b] \quad \frac{10^{1.5M}}{\eta_L(N_1)\,R^B} = 1.0$$

where $\eta_L(N_1)$ is the critical value of $\eta(N_1)$ at which liquefaction will take place.

Equation [15] can be simplified to allow for a ready appreciation of the mechanics of liquefaction. The term $\eta_L(N_1)$ is a function of soil resistance as measured by the SPT. It is called the liquefaction resistance function. The other functions involving M and R, both having influence on the energy arriving at the site, can be combined to form a function, $T(M, R)$, that reflects the intensity of the earthquake. Hence, $T(M, R)$ is called the seismic energy intensity function and is given by

$$[16] \quad T(M, R) = 10^{1.5M}/R^B$$

Liquefaction will take place when the seismic energy intensity function exceeds the liquefaction resistance function. This can be represented by

$$[17] \quad \frac{T(M, R)}{\eta_L(N_1)} \geq 1.0$$

The next task is to evaluate the functions T and η_L, by analysis of recorded observations made during past earthquakes.

Analysis of existing records

Two main sources of data were used in this analysis. The first was from the works of the University of California at Berkeley (Seed *et al.* 1975). This source listed 11 damaging earthquakes that occurred in the U.S.A., Japan, and Chile in the period 1802–1971. The earthquake magnitudes ranged from 5.5 to 8.4. A total of 38 sites was investigated for liquefaction or the lack of it.

The second source was from China (Xie 1984). Two major earthquakes were considered in which appropriate information was available. The 1976 devastating Tangshan earthquake killed 248 000 people. The magnitude was 7.8 and the hypocentre was at 11 km right beneath the city. The damage was extensive over a large area and 92 sites were studied. The other earthquake occurred in Haicheng in 1975, with a magnitude of 7.3. Six sites were considered from this earthquake.

For each site the following information was gathered: earthquake magnitude, hypocentre or epicentre location, soil type, depth of soil studied, depth of groundwater table, standard penetration resistance, hypocentre distance of the site, peak acceleration at the ground surface, average induced dynamic stress ratio, τ_{av}/σ_v', and identification of liquefaction occurrence. A data base was compiled for all 136 records. The appropriate information for the present analysis is shown in Tables 1 and 2. A summary of all the events is shown in Table 3.

Corrections for resistance from standard penetration test (SPT)

The standard penetration resistance (N) is the number of blows by a hammer of a standard weight required to drive a standard sampling tube 0.3 m into the ground. The value of N for a given soil, is, therefore, proportional to the energy delivered to the drill stem. As noted by Seed *et al.* (1985), this energy is affected by the energy delivery system, the shape of the hammer, and the procedures of operation. To standardize the input for determining the function $\eta_L(N_1)$, correction has to be made on the basis of efficiency of the energy delivered to the drill stem. As the majority of the field data in the U.S.A. were obtained using the safety hammer that develops 60% energy efficiency, Seed *et al.* (1985) suggested the following for standardizing the data:

$$[18] \quad N_{60} = \Psi N$$

TABLE 2. Site conditions and earthquake data from China for liquefaction study (after Xie 1984)

No.	Year	Magnitude	Hypocentre distance (km)	Type of sand*	Depth of sand (m)	Depth of water table (m)	SPT resistance N	Liquefied(?)	Site
1	1976	7.8	70.9	2	1.8	0.8	2	Yes	Tangshan
2	1976	7.8	69.5	1	4.1	1.0	5	Yes	Tangshan
3	1976	7.8	84.0	1	2.4	1.2	8	Yes	Tangshan
4	1976	7.8	84.0	2	1.3	0.8	6	Yes	Tangshan
5	1976	7.8	77.6	1	1.7	0.5	3	Yes	Tangshan
6	1976	7.8	71.9	1	2.1	1.6	8	Yes	Tangshan
7	1976	7.8	79.4	2	3.9	0.7	5	Yes	Tangshan
8	1976	7.8	81.6	1	3.3	1.1	7	Yes	Tangshan
9	1976	7.8	81.0	1	2.3	1.4	2	Yes	Tangshan
10	1976	7.8	82.9	2	6.3	1.1	9	Yes	Tangshan
11	1976	7.8	81.9	1	4.3	1.4	9	Yes	Tangshan
12	1976	7.8	81.9	2	1.8	1.2	4	Yes	Tangshan
13	1976	7.8	82.5	1	4.3	1.1	7	Yes	Tangshan
14	1976	7.8	81.7	1	2.3	1.2	6	Yes	Tangshan
15	1976	7.8	92.7	1	1.8	0.6	2	Yes	Tangshan
16	1976	7.8	91.7	1	2.3	0.7	1	Yes	Tangshan
17	1976	7.8	103.6	2	3.3	0.9	9	Yes	Tangshan
18	1976	7.8	117.5	1	9.5	2.0	6	No	Tangshan
19	1976	7.8	117.5	1	6.3	3.1	12	No	Tangshan
20	1976	7.8	83.3	1	2.3	1.6	9	No	Tangshan
21	1976	7.8	61.8	1	6.6	1.5	23	No	Tangshan
22	1976	7.8	64.4	1	8.6	2.0	10	No	Tangshan
23	1976	7.8	82.7	2	15.0	1.2	21	No	Tangshan
24	1976	7.8	74.8	1	4.3	0.7	16	No	Tangshan
25	1976	7.8	79.8	1	3.6	1.3	19	No	Tangshan
26	1976	7.8	82.5	1	2.0	1.0	9	No	Tangshan
27	1976	7.8	81.9	1	4.3	1.0	12	No	Tangshan
28	1976	7.8	81.9	2	8.8	1.0	14	No	Tangshan
29	1976	7.8	84.0	2	3.3	1.0	19	No	Tangshan
30	1976	7.8	91.3	1	3.9	0.6	10	No	Tangshan
31	1976	7.8	58.8	1	4.3	2.5	9	No	Tangshan
32	1976	7.8	50.2	2	4.8	1.0	14	No	Tangshan
33	1976	7.8	43.4	2	14.4	0.6	16	No	Tangshan
34	1976	7.8	116.5	1	8.7	1.6	8	Yes	Tangshan
35	1976	7.8	116.5	1	5.8	3.3	5	Yes	Tangshan
36	1976	7.8	117.5	1	9.2	1.1	12	Yes	Tangshan
37	1976	7.8	117.5	2	5.1	3.0	9	Yes	Tangshan
38	1976	7.8	117.5	1	7.2	3.2	8	Yes	Tangshan
39	1976	7.8	66.9	1	3.3	2.3	9	Yes	Tangshan
40	1976	7.8	64.9	1	2.3	2.2	4	Yes	Tangshan
41	1976	7.8	65.5	1	5.3	2.3	10	Yes	Tangshan
42	1976	7.8	66.2	2	2.3	2.5	4	Yes	Tangshan
43	1976	7.8	67.3	1	5.3	2.9	9	Yes	Tangshan
44	1976	7.8	44.9	1	1.3	0.6	8	Yes	Tangshan
45	1976	7.8	41.5	1	3.3	3.0	12	Yes	Tangshan
46	1976	7.8	45.6	1	4.3	1.3	1	Yes	Tangshan
47	1976	7.8	46.3	1	5.3	1.1	6	Yes	Tangshan
48	1976	7.8	45.4	2	9.4	0.7	11	Yes	Tangshan
49	1976	7.8	41.5	2	8.4	0.6	11	Yes	Tangshan
50	1976	7.8	32.9	2	2.9	1.0	7	Yes	Tangshan
51	1976	7.8	45.4	2	5.3	0.6	1	Yes	Tangshan
52	1976	7.8	42.5	1	2.6	1.5	6	Yes	Tangshan
53	1976	7.8	71.8	1	12.3	2.3	13	No	Tangshan
54	1976	7.8	48.3	1	3.4	2.0	8	No	Tangshan
55	1976	7.8	116.5	1	13.8	3.3	17	No	Tangshan
56	1976	7.8	115.5	2	9.1	3.8	17	No	Tangshan
57	1976	7.8	117.5	2	11.9	1.5	26	No	Tangshan
58	1976	7.8	40.2	1	1.3	1.1	15	No	Tangshan
59	1976	7.8	38.6	1	3.3	2.8	16	No	Tangshan
60	1976	7.8	45.6	1	4.3	3.1	15	No	Tangshan
61	1976	7.8	27.3	1	9.3	3.1	51	No	Tangshan
62	1976	7.8	24.6	1	2.6	0.4	10	Yes	Tangshan

TABLE 2 (*concluded*)

No.	Year	Magnitude	Hypocentre distance (km)	Type of sand*	Depth of sand (m)	Depth of water table (m)	SPT resistance N	Liquefied(?)	Site
63	1976	7.8	24.6	1	2.7	1.0	9	Yes	Tangshan
64	1976	7.8	24.6	1	4.5	1.1	22	Yes	Tangshan
65	1976	7.8	33.3	1	5.8	3.6	18	Yes	Tangshan
66	1976	7.8	33.3	1	4.4	3.5	13	Yes	Tangshan
67	1976	7.8	23.7	1	5.1	1.3	4	Yes	Tangshan
68	1976	7.8	23.7	1	5.0	1.0	10	Yes	Tangshan
69	1976	7.8	24.6	1	3.3	2.4	11	Yes	Tangshan
70	1976	7.8	16.3	2	5.9	1.0	9	Yes	Tangshan
71	1976	7.8	18.6	2	6.8	1.2	15	Yes	Tangshan
72	1976	7.8	14.2	1	8.6	1.9	7	Yes	Tangshan
73	1976	7.8	15.6	1	3.3	0.8	14	Yes	Tangshan
74	1976	7.8	20.3	1	3.8	0.6	4	Yes	Tangshan
75	1976	7.8	14.8	1	2.3	1.0	11	Yes	Tangshan
76	1976	7.8	16.7	2	1.8	1.0	7	Yes	Tangshan
77	1976	7.8	17.0	1	3.6	1.3	16	Yes	Tangshan
78	1976	7.8	16.7	2	6.4	1.5	16	Yes	Tangshan
79	1976	7.8	17.0	2	3.7	1.5	5	Yes	Tangshan
80	1976	7.8	14.2	2	5.4	1.4	5	Yes	Tangshan
81	1976	7.8	21.1	1	20.0	5.6	45	No	Tangshan
82	1976	7.8	21.1	2	14.8	5.3	73	No	Tangshan
83	1976	7.8	17.8	1	13.5	5.0	64	No	Tangshan
84	1976	7.8	17.8	1	9.3	4.9	61	No	Tangshan
85	1976	7.8	15.6	1	6.4	5.9	14	No	Tangshan
86	1976	7.8	20.9	2	6.4	2.3	18	No	Tangshan
87	1976	7.8	15.6	1	10.2	5.7	34	No	Tangshan
88	1976	7.8	24.6	1	4.0	1.8	12	No	Tangshan
89	1976	7.8	14.6	1	8.3	3.5	31	No	Tangshan
90	1976	7.8	15.6	1	4.5	4.5	22	No	Tangshan
91	1976	7.8	15.6	1	7.3	4.5	18	No	Tangshan
92	1976	7.8	15.6	1	9.9	5.5	30	No	Tangshan
93	1975	7.3	65.7	1	5.2	1.5	6	Yes	Haicheng
94	1975	7.3	65.7	1	6.4	1.5	6	Yes	Haicheng
95	1975	7.3	65.7	2	7.0	1.5	6	Yes	Haicheng
96	1975	7.3	43.7	2	10.5	1.5	11	Yes	Haicheng
97	1975	7.3	60.9	2	8.0	1.0	15	No	Haicheng
98	1975	7.3	60.9	2	12.0	1.0	20	No	Haicheng

*1 for sand, 2 for silty sand.

TABLE 3. Summary of data base for seismic liquefaction cases (1802–1976)

No.	Country	No. of earthquakes	Liquefied cases	Nonliquefied cases
1	U.S.A.	4	12	1
2	Japan	6	12	10
3	Chile	1	2	1
4	China	2	59	39
Total		13	85	51

where N_{60} = SPT resistance standardized to 60% energy efficiency,

[19] $\Psi = \mathrm{ER}/60$

and ER = energy efficiency of SPT system from which the uncorrected resistance N was obtained. Such a standardization has been used in the analysis in the present paper. Since data from the U.S.A., Chile, Japan, and China were used, the following briefly describes the appropriate corrections.

According to Seed *et al.* (1985), the practice of SPT in the U.S.A. and in most Pan-American countries yields the following: for a safety hammer used with 2 wraps of a rope around a pulley, $\Psi \cong 1.0$; for a donut hammer used with 2 wraps of a rope around a pulley, $\Psi \cong 0.75$.

Kovacs and Salomone (1984) and Seed *et al.* (1985) have compared the SPT in the U.S.A. and in Japan. They showed that the energy efficiency from the SPT in Japan is higher than that in the U.S.A. However, the Japanese practice adopts a significantly slower frequency and a smaller drill hole. The combined effects for loose to medium dense sand lead to $\Psi = 1.17$ for a donut hammer with free-fall release, and $\Psi = 1.0$ for a donut hammer with special throw release.

Experience of the use of SPT in China was summarized by Huang (1982) and Seed *et al.* (1985). Prior to 1975, the Chinese SPT hammers were operated manually with the rope and pulley method. The corresponding Ψ is equal to 0.83. More recently, Chinese engineers generally use an automatic mechanical trip to release the hammer. This yields an energy efficiency of about 60%; hence Ψ is equal to 1.0.

After correction for energy and operational variations, the SPT resistance also requires a correction for the effective overburden pressure, σ'_v. An arbitrary reference σ'_v = 100 kPa was used here as proposed by Seed *et al.* (1983) and the following correction applies:

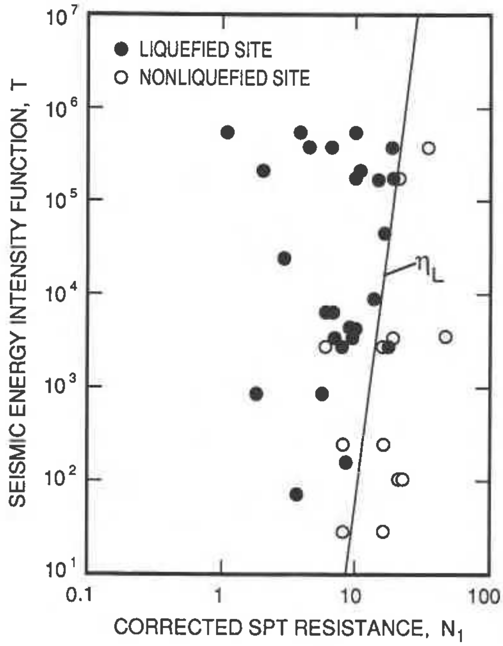

FIG. 6. Correlation of seismic energy intensity function with corrected SPT resistance from the data of Seed *et al.* (1975).

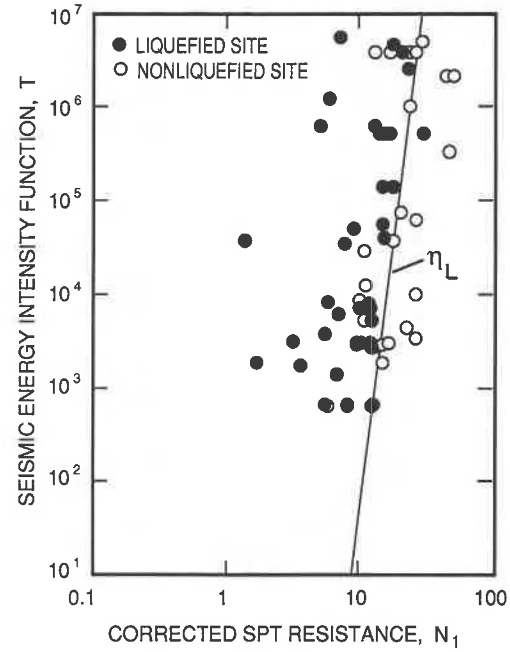

FIG. 7. Correlation of seismic energy intensity function with corrected SPT resistance for sand sites from the Chinese data (Xie 1984).

[20] $N_1 = C_N N_{60}$

where C_N = a function of σ_v' at the depth where the penetration test was conducted. Typical values of C_N were given by Seed *et al.* (1983). The fully corrected N_1 value was used in establishing the $\eta_L(N_1)$ function.

Parameter B *for earthquake intensity function*

The determination of the earthquake intensity function as defined by [16] requires the evaluation of parameter B. This parameter describes the attenuation characteristics of the seismic energy as expressed in [10]. For a highly fractured rock mass, the energy absorption is high. The corresponding energy attenuation will be high and the B value will be large. On the other hand, when the rock mass is intact, the B value will be low.

Hasegawa *et al.* (1981) summarized existing information and proposed a mean B value of 4.3 ± 0.5 for western Canada and western U.S.A., where highly fractured rock prevails. A $B = 4.3$ was chosen for the present study, as all the field data are from regions of highly fractured rock mass. Hence

[21] $T(M, R) = 10^{1.5M}/R^{4.3}$

where R is in kilometres.

Analysis of data of Seed et al. *(1975)*

This set of data is plotted in Fig. 6. On the basis of the treatment of the data by Seed *et al.* (1975) and Seed *et al.* (1983), the overwhelming majority of the sites can be considered as composed of sand. Both T and N_1 are shown on a logarithmic scale. Each filled circle represents a case of liquefaction failure, while each unfilled circle represents a nonliquefied site. A straight line is drawn to define the boundary separating the liquefied and nonliquefied sites. This line, therefore, mathematically corresponds to the equation for the condition of liquefaction and be written as

[22] $\eta_L(N_1) = 2.28N_1^{11.5} \times 10^{-10}$

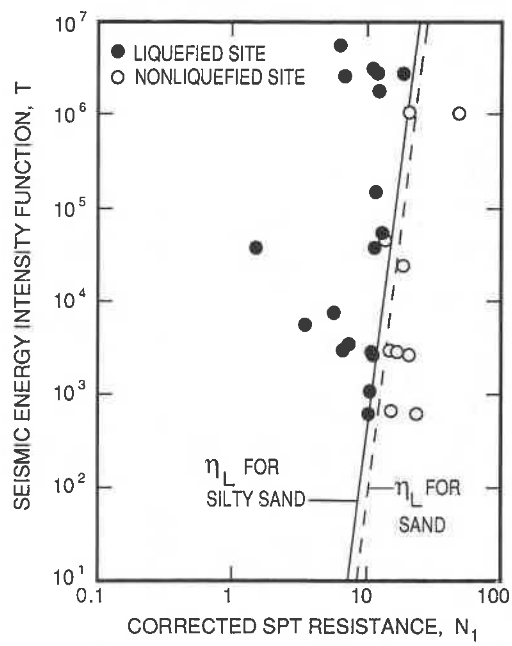

FIG. 8. Correlation of seismic energy intensity function with corrected SPT resistance for silty sand sites from the Chinese data (Xie 1984).

Substituting [22] and [21] into [17], one obtains

[23] $$\frac{T(M, R)}{\eta_L(N_1)} = \frac{10^{1.5M}}{2.28N_1^{11.5} \times 10^{-10} \times R^{4.3}} \geq 1$$

Analysis of Chinese data

The Chinese data (Table 2) show that a significant number of sites are located on silty sand, which behaves differently from sand. The data, therefore, warrant a separation of these two materials for a more accurate definition of $\eta_L(N_1)$. The data for sand are plotted in Fig. 7. Again, a line

TABLE 4. Comparison of success rates on predicting liquefaction events by the present energy method and by the stress method of Seed *et al.* (1983)

Data source	Sand type	No. of sites	Success rate by energy method (%)	Success rate by stress method (%)
Seed *et al.* (1975)	Sand	38	89	87
Xie (1984)	Sand	65	82	71
Xie (1984)	Silty sand	33	97	66

can be drawn to divide the liquefied and nonliquefied sites. This line is identical to that for the data described in the previous section.

Figure 8 plots the data for the silty sand sites. A similar line can also be drawn to distinguish the liquefied sites from the nonliquefied ones. The mathematical expression for this line, however, is different from that for sand. It is given by

[24] $\eta_L(N_1) = 1.14 \times N_1^{11.5} \times 10^{-9}$

This liquefaction resistance function implies that silty sand can withstand a higher earthquake intensity than sand of the same resistance N_1. This is probably due to the cohesiveness of the silty component that enhances the dynamic resistance of the silty sand. According to Zhou (1981), the silty sand found near Tangshan is composed of about 60% silt-size particles or less and about 14% clay.

Comparison of energy method and stress method

The present method is simpler to apply than the method by Seed *et al.* (1983). The present method requires the values of R and M. For an earthquake that has taken place, these two quantities can now be reasonably determined. For design purposes, however, these quantities have to be predicted using a probabilistic approach that is readily available in the open literature (e.g., Basham *et al.* 1982). As soon as these quantities are obtained, along with the N_1 values, the liquefaction potential of a site can be examined based on [17].

The stress method of Seed *et al.* also requires evaluation of two quantities of an earthquake: peak horizontal acceleration of the bedrock (a_m) and magnitude (M). The process of determination of a_m and M is similar to that of the present method. After evaluation, however, these values cannot be applied directly to examine the liquefaction potential of a site, assuming N_1 is known. Two more steps are required. First, the peak horizontal acceleration at the ground surface has to be estimated using a_m with due regard to soil amplification or attenuation of vibration as mentioned earlier. This change of ground motion characteristics depends on the geometry and properties of the soil layers. Second, this method is based on observations of earthquakes of M approximately equal to 7.5. Estimation of liquefaction potential at other magnitudes is based on a laboratory study to yield a curve showing the liquefaction resistances at various numbers of cycles of loading. This curve then provides correction factors for application of values of M other than 7.5.

The use of the energy concept in the present study is unambiguous compared with the acceleration concept in the stress method. Energy is a scalar and as such there is no need to determine any direction. Acceleration is a vector with two horizontal components and a vertical component. Only the maximum value of horizontal acceleration is used and the vertical component is ignored in the stress method. There is a growing appreciation of a significant vertical component (e.g., Atkinson 1986) that many have bearing on the stress method.

The present energy method is more reliable than the stress method. It should be noted that both methods produce curves for examining the likelihood of liquefaction failure for sand and for silty sand. While the energy method is based on the Chinese data and the data of Seed *et al.* (1975), the stress method is based also on the data of Seed *et al.* (1975) and other data from Seed *et al.* (1983), who claimed that the stress method is applicable to the Chinese data. Therefore, application of both methods to the data base collected in this study will fairly reflect their relative reliability. A comparison of the results is shown in Table 4. For the first group of data from Seed *et al.* (1975), the success rates of correctly predicting the occurrence and nonoccurrence of liquefaction failure are 89% and 87% for the energy and the stress methods, respectively. For the Chinese data involving sand sites, the success rates of the energy method and the stress method are 82% and 71%, respectively. For the silty sand sites, the corresponding success rates are 97% and 66%, respectively. Therefore, the energy method has a higher rate of success in evaluating liquefaction potential.

A worked example

The use of [23] for analyzing liquefaction potential is illustrated with an example from the recent 1989 Loma Prieta (San Francisco) earthquake. The magnitude on the Richter scale of this earthquake is 7.1 and the focal depth is 18.5 km. This earthquake is considered the largest natural disaster in U.S. history, with estimated damage costs as high as U.S. $10 billion. Liquefaction failure was extensive (Astaneh *et al.* 1989). In the Marina district on the central part of the northern coast of San Francisco, the senior author noted at least 20 spots of sand boils during a site visit shortly after the earthquake. This district is 100 km away from the epicentre. The hypocentral distance R is therefore equal to $(100^2 + 18.5^2)^{1/2} = 101.7$ km. Substituting the values of R and M into [23], one obtains, for the condition of liquefaction failure, a corrected SPT resistance N_1 of less than 10.3.

The subsoil deposit of the Marina district is composed of a hydraulic fill placed on top of a thick layer of San Francisco Bay mud. The material of the sand boils is a dark gray uniform sand with occasional sea shells, indicating the hydraulic fill liquefied during the earthquake. Such a material having a value of N_1 less than 10.3 is not surprising.

Summary and conclusions

A study has been conducted to establish a method for site evaluation of liquefaction potential based on an energy approach. Cyclic triaxial and cyclic torsional simple shear tests have been conducted on a Fujian medium sand. The results were analyzed along with earthquake parameters to

derive a simple equation for determining liquefaction potential. The equation was applied to published records to evaluate the appropriate parameters and to test its validity. The following conclusions can be drawn from the study:
(1) A unique relationship exists between excess pore pressure and dissipated energy during cyclic loading on sand. This relationship, mathematically represented by [8], takes into account consolidation stress, consolidation ratio, and relative density.
(2) The unique relationship can be combined with an earthquake energy attenuation equation to yield a simple criterion, [17], for defining the condition of liquefaction. This criterion involves the use of earthquake magnitude, hypocentral distance, and the corrected resistance from the standard penetration test.
(3) Constants for the criterion have been determined based on 136 sites from 13 major earthquakes over the world.
(4) This energy method has been compared with the stress method by Seed *et al.* (1983). The comparison shows the energy method is simpler to apply and more reliable.

Acknowledgements

The authors express their sincere appreciation for the assistance of the geotechnical laboratory staff, Dalian University of Technology, China, in conducting the test program. The research was partly funded by Natural Sciences and Engineering Research Council of Canada operation grant No. A4387.

ASTANEH, A., BERTERO, V.V., BOLT, B.A., MAHIN, S.A., MOEHLE, J.P., and SEED, R.B. 1989. Preliminary report on the seismological and engineering aspects of the October 17, 1989 Santa Cruz (Loma Pireta) earthquake. Earthquake Engineering Research Center College of Engineering, University of California, Berkley, Report UCB/EERC-89/14.

ATKINSON, G.M. 1986. Ground motion for eastern North America. Ontario Hydro, Toronto, Ont., Report 86353.

BASHAM, P.W., WEICHERT, D.H., ANGLIN, F.M., and BERRY, M.J. 1982. New probabilistic strong seismic ground motion maps of Canada: a compilation of earthquake source zones, methods and results. Energy, Mines and Resources Canada, Earth Physics Branch, Open File 82-33.

DAVIS, R.O., and BERRILL, J.B. 1982. Energy dissipation and seismic liquefaction in sands. Earthquake Engineering & Structural Dynamics, **10**: 59–68.

GIBBS, H.J., and HOLTZ, W.G. 1957. Research on determining the density of sands by spoon penetration testing. Proceedings, 4th International Conference on Soil Mechanics and Foundation Engineering, London, vol. 1, pp. 35–39.

GUTENBERG, B., and RICHTER, C.F. 1956. Magnitude and energy of earthquakes. Annali di Geofisica, **9**: 1–15.

HASEGAWA, H.S., BASHAM, P.W., and BERRY, M.J. 1981. Attenuation relations for strong seismic ground motion in Canada. Bulletin of the Seismological Society of America, **71**: 1943–1962.

HE, G.N. 1981. Energy analysis procedure for evaluating liquefaction potential [in Chinese]. Chinese Journal of Geotechnical Enginering, **3**: 11–21.

HUANG, S.M. 1982. Experience on a standard penetration test. Proceedings, 2nd European Symposium on Penetration Testing, Amsterdam, vol. 1, pp. 61–66.

IWASAKI, T., TATSUOKA, F., TOKIDA, K., and YASUDA, S. 1978. A practical method for assessing soil liquefaction potential based on case histories at various sites in Japan. Proceedings, 2nd International Conference on Microzonation for Safer Construction—Research and Applications, vol. 2, pp. 885–896.

KOVACS, W.D., and SALOMONE, L.A. 1984. Field evaluation of SPT energy, equipment and methods in Japan compared with the SPT in the United States. National Bureau of Standards, U.S. Department of Commerce, NBS1E-2910.

MARTIN, G.R., FINN, W.D.L., and SEED, H.B. 1975. Fundamentals of liquefaction under cyclic loading. ASCE Journal of the Geotechnical Engineering Division, **101**: 423–438.

MURPHY, J.R., and O'BRIEN, L.J. 1977. The correlation of peak ground acceleration amplitude with seismic intensity and other physical parameters. Bulletin of the Seismological Society of America, **67**: 877–915.

NUTTLI, O.W. 1979. The relation of sustained maximum ground acceleration and velocity to earthquake intensity and magnitude. US Army Engineer Waterways Experiment Station, Miscellaneous Paper S-76-1, Report 16, p. 74.

SEED, H.B., and IDRISS, I.M. 1967. Analysis of soil liquefaction—Niigata earthquake. ASCE Journal of the Soil Mechanics and Foundations Division, **93**: 83–108.

——— 1971. Simplified procedure for evaluating soil liquefaction potential. ASCE Journal of the Soil Mechanics and Foundations Division, **97**: 1249–1273.

SEED, H.B., ARANGO, I., and CHAN, C.K. 1975. Evaluation of soil liquefaction potential during earthquake. Earthquake Engineering Research Center, University of California, Berkley, Report EERC75-28.

SEED, H.B., IDRISS, I.M., and ARANGO, I. 1983. Evaluation of liquefaction potential using field performance data. ASCE Journal of Geotechnical Engineering, **109**: 458–482.

SEED, H.B., TOKIMATSU, K., HARDER, L.F., and CHUNG, R.M. 1985. Influence of SPT procedure in soil liquefaction resistance evaluations. ASCE Journal of Geotechnical Engineering, **111**: 1425–1445.

STREET, R.L., and LACROIX, A. 1979. An empirical study of New England seismicity: 1727–1977. Bulletin of the Seismological Society of America, **69**: 159–175.

TATSUOKA, F., MURAMATSU, M., and SASAKI, T. 1982. Cyclic undrained stress-strain behaviour of dense sand by torsional simple shear test. Soils and Foundations, **22**: 55–70.

XIE, J.F. 1984. Some comments on the formula for estimating the liquefaction of sand in revised aseismic design code. China Earthquake Engineering and Engineering Vibration, **2**: 95–126.

ZHOU, S.G. 1981. Influence of fines on evaluating liquefaction of sand by CPT. International Conference on Recent Advances in Geotechnical Earthquake Engineering and Soil Dynamics, St. Louis, MO, vol. 1, pp. 167–172.